

## ANOMALIES IN TIME DELAYS OF LENSED GRAVITATIONAL WAVES AND DARK MATTER SUBSTRUCTURES

KAI LIAO<sup>1</sup>, XUHENG DING<sup>2</sup>, MAREK BIESIADA<sup>3,4</sup>, XI-LONG FAN<sup>5</sup> ZONG-HONG ZHU<sup>2,3</sup>

<sup>1</sup> School of Science, Wuhan University of Technology, Wuhan 430070, China.

<sup>2</sup> School of Physics and Technology, Wuhan University, Wuhan 430072, China.

<sup>3</sup> Department of Astronomy, Beijing Normal University, Beijing 100875, China.

<sup>4</sup> Department of Astrophysics and Cosmology, Institute of Physics, University of Silesia, 75 Pułku Piechoty 1, 41-500 Chorzów, Poland.

<sup>5</sup> Department of Physics and Mechanical and Electrical Engineering, Hubei University of Education, Wuhan 430205, China.

*Draft version September 20, 2018*

### ABSTRACT

The cold dark matter scenario of hierarchical large-scale structure formation predicts the existence of abundant subhalos around large galaxies. However, the number of observed dwarf galaxies is far from this theoretical prediction, suggesting that most of the subhalos could be dark or quite faint. Gravitational lensing is a powerful tool to probe the mass distribution directly irrespective of whether it is visible or dark. Time delay anomalies in strongly lensed quasar systems are complementary to flux ratio anomalies in probing dark matter substructure in galaxies. Here we propose that lensed gravitational waves detected by the third-generation ground detectors with quite accurate time delay measurements could be a much better tool for this study than conventional techniques. Combined with good quality images of lensed host galaxies identified by the electromagnetic counterpart measurements, lensed GW signals could make the systematic errors caused by dark matter substructures detectable at several percent levels, depending on their mass functions, internal distribution of subhalos and lensing system configuration.

*Subject headings:* lensing: strong - gravitational wave - dark matter

### 1. INTRODUCTION

The cold dark matter (CDM) model predicts that about 25% of the matter content in the Universe is of non-baryonic origin and large dark matter halos have been assembled hierarchically from smaller ones. While this model has successfully explained the large-scale structure of the Universe at the level of galaxies and galaxy clusters, its sub-galactic scale predictions have not yet been well tested. According to the simulations, a small part of galactic dark matter halos should be in the form of subhalos that temporarily survived from tidal stripping process. The mass function of these clumps approximately follows a power law function  $dN/dm \propto m^{-1.8}$  (Diemand et. al. 2008). It is believed that subhalos anchoring gas allowing for star formation would appear as satellite dwarf galaxies. Therefore, we are supposed to observe a lot of such satellites. However, the long-standing “Missing Satellite Problem” makes the picture blurred. The CDM simulations predict that thousands of subhalos should be bound to the Milky Way (Klypin et. al. 1999), while only  $\sim 10$  luminous satellites have been observed (Drlica-Wagner et. al. 2015). The same is true in the Andromeda M31 galaxy (Moore et. al. 1999).

To solve the mismatch between the low-mass end of the subhalo mass function and the luminosity function of dwarf galaxies, various mechanisms were proposed. For example, processes inhibiting star formation in low-mass subhalos, or observational biases that rule faint satellites out of the surveys. Another possibility is that substantial scatter exists among galaxies, i.e., the Milky Way and Andromeda are quite spe-

cial ones. Another approach was taken by theorists, who tried to modify dark matter properties to decrease the formation of low-mass subhalos. These ideas include: warm dark matter (Lovell et. al. 2014), self-interacting dark matter (Spergel & Steinhardt 2000), fuzzy dark matter (Wayne et. al. 2000) and super-WIMPs (Land & Magueijo 2005). Inflation was also adjusted to reduce the low-mass end of subhalos (Kamionkowski & Liddle 2000). Therefore, measuring the subhalo mass function and how does it vary with the environment are quite important questions, essential for both basic physics and astrophysics.

Strong gravitational lensing is an excellent tool to directly detect substructure in galaxies outside the local group (Mao & Schneider 1998; Zackrisson et. al. 2010), since it does not distinguish between luminous and dark matter. Lensed quasar systems have been used to detect dark matter substructure using the observed flux ratio anomalies. In many cases, while the smooth lens model can fit the image positions well, yet flux ratios among images become anomalous most probably due to the substructure in the lensing galaxy dark matter halos. The smooth model here, can not be formulated non-parametrically in terms of the multipole expansion, since in such case it would lead to unrealistic galaxy shapes (Keeton & Moustakas 2009). On the other hand, with a parametric smooth model, one can infer the properties of subhalos. However, this approach may suffer from propagation effects in the interstellar medium (Mittal et. al. 2007) and microlensing effects by the motion of stars in the lensing galaxy (Schechter & Wambsganss 2002). Selecting different wavelengths can effectively mitigate these biases (Jackson et. al. 2015; Nierenberg et. al. 2017). Be-

sides, the astrometric effects (Koopmans et. al. 2002; Vegetti & Koopmans 2008) or the small-scale structure in macro-images (Inoue & Chiba 2005) could also be utilized to study dark matter substructure.

Keeton and Moustakas (Keeton & Moustakas 2009) proposed that time delay perturbations between macro-images could complement the methods mentioned above by measuring different moments of the substructure mass function and applied it to well studied lensed quasar systems RX J1131-1231 and B1422+231 (Congdon et. al. 2010). This approach is immune to dust extinction or stellar microlensing. Note that image positions and flux ratios depend on the first and the second derivatives of the lens potential, respectively, while time delay depends directly on the lens potential.

To achieve a robust identification of time delay anomalies, one needs to simultaneously improve accuracies of both the smooth model and the measurements of time delays. However, the light curves of lensed quasars allow for at most  $\sim 3\%$  accuracy of time delays (Liao et. al. 2015), while the typical perturbation is only a fraction of a day (Keeton & Moustakas 2009). Recently, (Tie & Kochanek 2018) suggested that a new microlensing effect on time delays based on differential magnification of the accretion disc of the lensed quasar, may further increase the uncertainties up to 30%. Besides, smooth model uncertainties in lensed quasars were based on the assumption of point sources and Monte Carlo simulation based on specific galaxy catalogs (Congdon et. al. 2010). Therefore, they could mask the time delay perturbations. Consequently, one might doubt, whether the anomalies found in RX J1131-1231 and B1422+231 were directly related with dark matter subhalos.

Recent detections, by the Advanced Laser Interferometer Gravitational Wave Observatory (aLIGO), of gravitational wave (GW) signals generated in mergers of binary black holes (BHs) opened a new window on the Universe (Abbott et. al. 2016a,b, 2017a). Lensing of GW by intervening masses (galaxies) have been discussed by (Wang et. al. 1996; Nakamura 1998; Takahashi & Nakamura 2003; Cao et. al. 2014; Sereno et. al. 2010). Furthermore, the observed electromagnetic (EM) counterpart of the binary neutron stars merger opened a new chapter in the multi-messenger astronomy (Abbott et. al. 2017b). The next generation of GW interferometric detectors, like the Einstein Telescope (ET) will broaden the accessible volume of the Universe by three orders of magnitude with forecasted tens to hundreds of thousands of detections per year (Abernathy et. al. 2011) leading to expectation that many of the sources could be gravitationally lensed. This was discussed by (Piórkowska et. al. 2013; Biesiada et. al. 2014; Ding et. al. 2015) with a conclusion that ET should register about 50 – 100 strongly lensed inspiral events per year, thus providing a considerable catalog of such events during a few years of its successful operation. Lensed GW signals accompanied by EM counterparts are supposed to be valuable in the context of both the fundamental physics (Fan et. al. 2017) and cosmology (Liao et. al. 2017).

In this paper, we propose to use lensed gravitational wave signals together with their electromagnetic counterparts to identify time delay anomalies and study dark

matter substructure. **For simplicity, we attribute all anomalies to the dark matter substructure. However, we emphasize that for some realistic systems, complex baryonic structure can also contribute to the observed anomalies (Hsueh et. al. 2016, 2017). Ignoring the full complexity of the lens macro-model would overestimate the dark matter substructure component (Xu et. al. 2015; Gilman et. al. 2017; Evans & Witt 2003).** Despite of this, our analysis shows that systematic uncertainties caused by dark matter subhalo perturbations can be detected to some percent levels, depending on the subhalo mass function, internal structure of subhalos, and lensing system configuration.

## 2. SYSTEMATICS BY DARK MATTER SUBSTRUCTURE

According to gravitational lensing theory (Treu 2010), time delay between multiple images  $i, j$  is given by:

$$\Delta t_{i,j} = \frac{D_{\Delta t}(1+z_d)}{c} \Delta \phi_{i,j}, \quad (1)$$

where  $c$  is the speed of light,  $\Delta \phi_{i,j} = [(\theta_i - \beta)^2/2 - \psi(\theta_i) - (\theta_j - \beta)^2/2 + \psi(\theta_j)]$  is the Fermat potential difference for image angular positions  $\theta_i$  and  $\theta_j$ ;  $\beta$  denotes the source position, and  $\psi$  is the two-dimensional lensing potential determined by the surface mass density of the lens  $\kappa$  in units of critical density  $\Sigma_{\text{crit}} = c^2 D_s / (4\pi G D_d D_{ds})$  through the Poisson equation  $\nabla^2 \psi = 2\kappa$ ,  $D_d$ ,  $D_s$  and  $D_{ds}$  are angular diameter distances to the lens (deflector) located at redshift  $z_d$ , to the source located at redshift  $z_s$  and between them, respectively. Dark matter substructure could perturb Fermat potentials including gravitational potential and image positions and therefore could perturb time delays.

Lensed GW signals accompanied by electromagnetic counterparts, in particular kilonovae that are relatively stable and easy to observe (Fernández & Metzger 2016), are especially advantageous for studying the dark matter substructure. Firstly, time delay measured by GWs could be quite accurate due to the transient nature of the event. They can be determined with accuracy  $\sim 0.1s$  (Fan et. al. 2017), and such measurement is essentially waveform independent. Secondly, the kilonovae last only for months, so one could measure the entire host galaxy arcs before or after the electromagnetic counterpart, which strongly facilitates lens modelling (Liao et. al. 2017). In addition to the analysis of (Keeton & Moustakas 2009), time delay measurements should be not affected by microlensing due to the long wavelengths of GWs in the diffraction limit (Takahashi & Nakamura 2003).

Time delays of lensed GW signals observed together with their electromagnetic counterparts are affected by at least five types of uncertainties. First, is the combined observational uncertainty  $\sigma_{\text{obs}}$  comprising pixel intensities, central velocity dispersion and point image positions. Time delay measurements are not included since we assume they would be determined accurately with the GW signals. This component can be thought of as the smooth lens model uncertainty. Next is  $\sigma_{\text{LOS}}$  arising from the mass density fluctuation along the line of sight. Then, the uncertainty  $\sigma_{\text{cosm}}$  stemming from the cosmological model adopted in calculations of distances should

be taken into account. It captures a possible mismatch between the true and fiducial background cosmological model. The fourth component  $\sigma_{dm}$  is directly caused by dark matter subhalo perturbations. Note that astrometric effects are included here because we measure time delays of the perturbed images. The last component is  $\sigma_{arc}$  due to the perturbation of images (arcs) by dark matter halos. This systematic component would in turn affect the accuracy of the smooth lens model. The total uncertainty is given by:

$$\sigma_{tot}^2 = \underbrace{\sigma_{obs}^2 + \sigma_{LOS}^2 + \sigma_{cosm}^2}_{\sigma_{stat}^2} + \underbrace{\sigma_{arc}^2 + \sigma_{dm}^2}_{\sigma_{sys}^2}, \quad (2)$$

$\sigma_{tot}$  can be seen as the difference between the measured time delay and the one inferred from the smooth lens model best fitted to images. From the perspective of dark matter substructure we propose to treat the first three terms collectively as statistical uncertainties, even though some of them are in fact systematics (but due to effects different from the one we are focused on). In this convention, the last two components are systematic ones — caused by dark matter halos resulting in apparent anomalies. Note that  $\sigma_{dm}$  is correlated with  $\sigma_{arc}$ . However, as we will discuss later, this correlation could be neglected.

Since we assume that measurements of time delays by GW signals are accurate, the corresponding extra uncertainty is  $\sigma_{\Delta t} = 0$ . If applied to lensed quasars, one would need to consider additional 3% uncertainty of  $\Delta t$  from light curves and moreover  $\sigma_{obs}$  would be larger due to the bright AGNs contaminating the arcs.

**One should also include another systematic uncertainty from the selection of smooth macro model. For example, a power-law model and a composite model give different results (Wong et. al. 2017). However, this systematics should not exceed the scale of  $\sigma_{obs}$  and can be well controlled according to current techniques (Wong et. al. 2017; Suyu et. al. 2013, 2017). Therefore, we do not include it explicitly in this work assuming that  $\sigma_{obs}$  is sufficient.**

### 3. SIMULATIONS AND RESULTS

In order to illustrate our idea, we investigate  $\sigma_{dm}, \sigma_{obs}, \sigma_{arc}$  for the fiducial double and quad systems, respectively. The other two uncertainties  $\sigma_{LOS}$  and  $\sigma_{cosm}$  are estimated from different inputs, so in both cases we take them as 2% and 1%, respectively (Rusu et. al. 2017).

#### 3.1. Reference lensing system

**In principle, a realistic approach capable of revealing more potential systematics should be based on numerical simulations of the lens. However, in order to illustrate our idea we only use a simple macro model. We refer to the ongoing work (Ding et. al. 2018), where the Time Delay Lens Modelling Challenge (TDLMC) program will thoroughly investigate systematic errors and biases of the lens model, with the purpose to check whether precision could dominate systematics in current lensing techniques.**

To show how time delay anomalies are related to dark matter substructure, we focus on a specific lensing system with the source and the lens redshifts 1.5 and 0.5, respectively. The reference smooth lens galaxy is modeled by a singular isothermal ellipsoid (SIE), with three-dimensional radial profile  $\rho(r) \propto r^{-2}$ , central velocity dispersion  $\sigma_v = 300 \text{ km/s}$ , ellipticity  $e = 0.2$  and orientation  $\theta_e = 45^\circ$ . Besides, we add a constant shear modelling the impact of the lens environment: the amplitude is 0.003 with orientation  $\theta_\gamma = 120^\circ$ .

The reference host galaxy of the source is modeled by the Sérsic model, where the projected mass profile is:

$$\Sigma(r) = \frac{M_{tot}}{\pi r_s^2 \Gamma(2n+1)} e^{-(\frac{r}{r_s})^{1/n}}, \quad (3)$$

where  $M_{tot}$  is the total mass and is proportional to the total brightness  $L_{tot}$ ,  $r_s$  is the scale radius related to the effective radius  $r_e$  and the Sérsic index,  $\Gamma(z)$  is the Euler's Gamma function,  $n$  is the Sérsic index controlling the concentration:  $n = 1$  corresponds to exponential disk,  $n = 4$  corresponds to de Vaucouleurs profile. We assume  $L_{tot} = 250, e = 0.3, \theta_e = 120^\circ, r_e = 0.35'', n = 2$ . The source was put at two positions:  $\beta = (0.15'', 0.05'')$  and  $\beta = (0.05'', 0.05'')$  so that it can form double image and quadruple image systems. Fig. 1 (a) (b) (c) shows the lensed host galaxy images and the unlensed one, all are without noise, in one second exposure time.

#### 3.2. Subhalo population and $\sigma_{dm}$

According to the CDM simulations, dark matter subhalo mass function approximately follows a power law,  $dN/dM \propto m^\beta$  with  $\beta \approx -1.8$ . For simplicity and the purpose of illustration, we assume that dark matter subhalos trace the total mass,  $\kappa_s(r) = f_s \kappa_{tot}(r)$ . We also consider finite range of subhalo mass. For the case 1,  $f_s = 0.01$ , we choose  $10^7 M_{sun} < m < 10^9 M_{sun}$  and assume the subhalos are modelled by point mass. For the case 2,  $f_s = 0.01$ , we assume that the subhalos have internal structure modelled by pseudo-Jaffe model, the respective parameters of which are shown in Tab 1. For case 3,  $f_s = 0.001$ , we choose  $10^6 M_{sun} < m < 10^8 M_{sun}$  modelled by point mass. More examples of realistic mass functions, can be found in (Keeton & Moustakas 2009). To illustrate the impact of subhalo mass and dark matter fraction, we considered cases 1 and 2 for double-image system, and cases 2 and 3 for quad system.

Using publicly available lensing software “glafic” (Oguri 2010), we first calculated the distribution of convergence  $\kappa(r)$  and then converted it to surface mass density. We assumed that  $f_s$  of the total mass within two Einstein radii is in dark matter. We randomly put these subhalos in the lens plane. Fig. 2 shows the critical lines for three cases mentioned above, in order to illustrate the impact of dark matter perturbations.

We simulated  $10^4$  realizations of lensing systems affected by dark matter subhalos by randomly choosing the subhalo positions. For each realization, we calculated time delays between images. In rare cases, certain images might split up. This phenomenon has been studied as an effect of small-scale structure. However, we focus on time delay anomalies and we ignored it. We also noticed that for some cusp image systems, the order

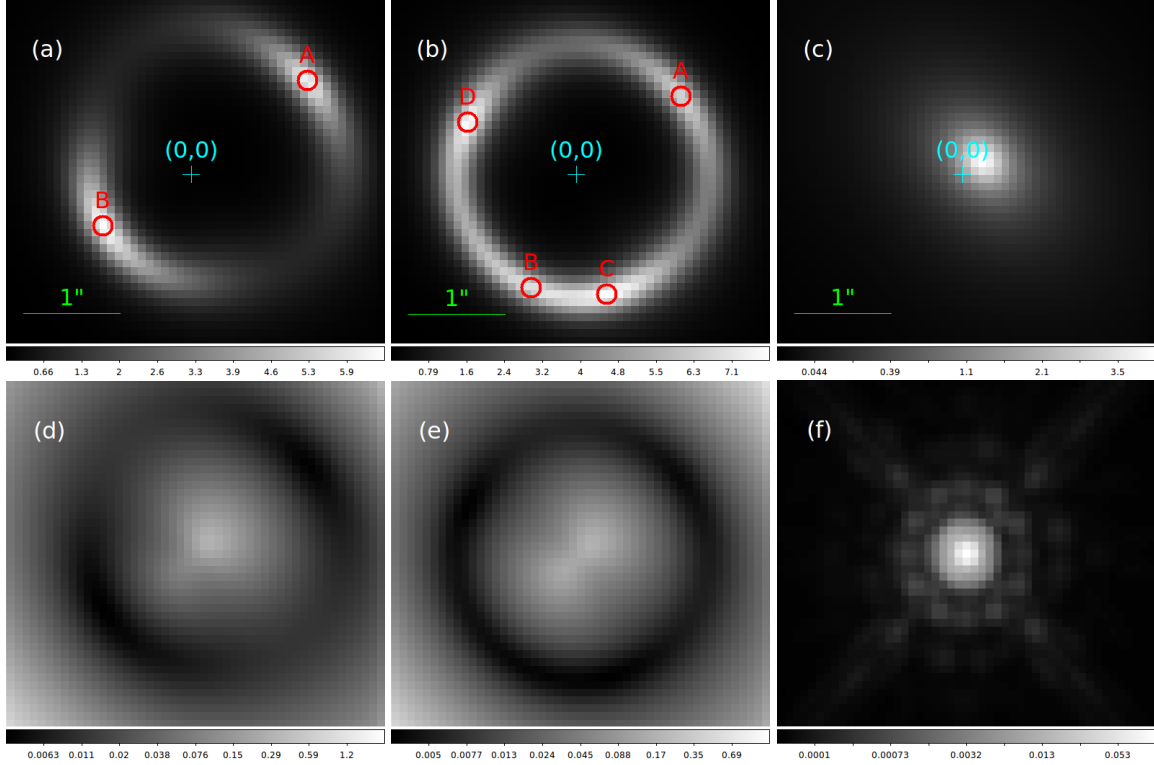


FIG. 1.— (a) simulated host arc image of double-image system without dark matter subhalo perturbation and noise; (b) simulated host arc image of quad-image system without dark matter subhalo perturbation and noise; (c) original source image without lensing; (d) relative noise map for double-image system; (e) relative noise map for quad-image system; (f) PSF image based on F160W from TINY TIM.

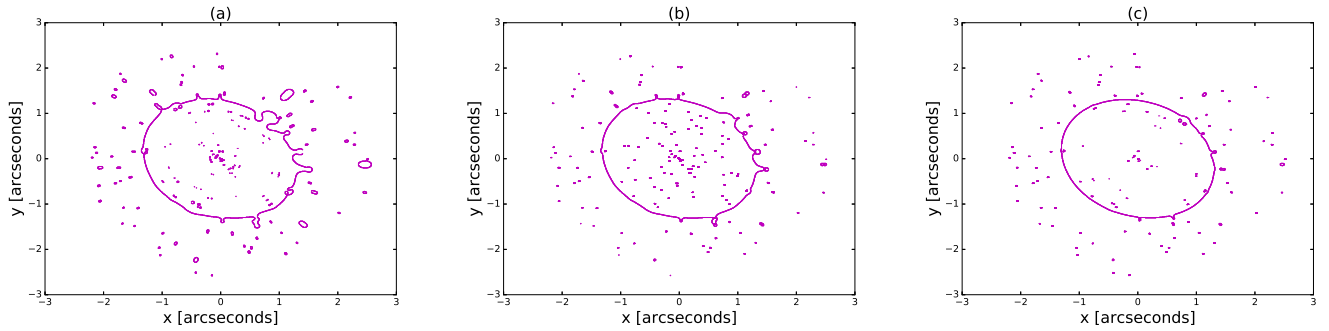


FIG. 2.— Perturbed critical lines for different mass functions and internal structures. (a) case 1; (b) case 2; (c) case 3.

$m/M_{sun}$	$\sigma(km/s)$	$r_{trun}(\prime\prime)$	$r_{core}(\prime\prime)$	$r_{cin}^{jaffe}(\prime\prime)$	$r_{cin}^{point}(\prime\prime)$
7.76e+07	19.5	0.05	0.002	0.0034	0.0202
4.57e+07	19.7	0.03	0.002	0.0032	0.0155
2.69e+07	17	0.024	0.002	0.0012	0.0119
1.58e+07	15.3	0.017	0.001	0.0023	0.0091
1.31e+08	20	0.08	0.002	0.0039	0.0263
2.23e+08	26	0.08	0.002	0.0082	0.0342
3.80e+08	35.1	0.08	0.007	0.0086	0.0446
6.45e+08	36.4	0.123	0.008	0.0092	0.0581
1.09e+09	46.2	0.13	0.01	0.0186	0.0757

TABLE 1

TYPICAL PARAMETER VALUES USED TO MODEL SUBHALOS WITH PSEUDO-JAFFE ELLIPTICAL MODEL  $\rho \propto (r^2 + r_{core}^2)^{-1}(r^2 + r_{trun}^2)^{-1}$ , WHERE  $m$  IS THE SUBHALO MASS,  $\sigma$  IS THE CENTRAL VELOCITY DISPERSION. WE CALCULATED EINSTEIN RADII FOR BOTH THE EXTENDED STRUCTURE AND THE POINT MASS.

of arrival changed. Based on simulations we calculated the standard deviation of all perturbed time delays and treated it as  $\sigma_{dm}$ . Fig. 3 (a) and (d) show the corresponding histograms. Note that the image positions were also perturbed as shown in Fig. 4 and Tab. 2.

### 3.3. Mock observations

Simulation of images is based on the state-of-the-art H0LiCOW project standard (Ding et. al. 2017). We assumed that images are taken by the Hubble Space Telescope (HST) with the Wide Field Camera 3 (WFC3) IR channel in the F160W band. The corresponding PSF generated by Tinytim<sup>1</sup> is shown in Fig. 1 (f). Following common practice, we adopted eight dithered images and stacked them into a final image; the pixel size is  $0.13''$  to  $0.08''$ , before and after drizzling. We added noise according to the realistic observation, including background, read noise and Poisson noise shown in Fig. 1 (d) for double and (e) quad systems. Total exposure time was assumed as  $1200s \times 8 = 9600s$ . For details of the simulation, see (Ding et. al. 2017) and (arxiv/1801.01506). Besides, we assume astrometric uncertainty as  $0.005''$  and velocity dispersion uncertainty as  $6.5\%$  (Wong et. al. 2017).

### 3.4. Best fits and $\sigma_{obs}$

In order to fit the lens model to observations of arcs, velocity dispersion and image positions, we used a power law model with the radial profile  $\rho(r) \propto r^{-\gamma}$  plus shear. Note that in this process, we did not use the measurements of time delays from GWs. There were 17 free parameters consisting of source position (2), lens position (2), lens model parameters (6), host galaxy parameters (7). For different noise realizations, we fitted parameters of the lens and source positions to find the best smooth lens model and then we inferred corresponding time delays. To avoid local trapping of free parameters during optimization process, we randomized the initial model parameter values, though it would take a longer time to find the global minimum of the objective function. The posterior PDF of model parameters  $\xi$  mentioned above can be expressed as:

$$P(\xi | \mathbf{I}, \sigma_v, \boldsymbol{\theta}) \propto P(\mathbf{I}, \sigma_v, \boldsymbol{\theta} | \xi) P(\xi), \quad (4)$$

where  $\mathbf{I}$  stands for the pixel intensities of arcs,  $\boldsymbol{\theta}$  stands for the point image positions. The likelihood can be further written as a product of Gaussian distributions:  $P(\mathbf{I})P(\sigma_v)P(\boldsymbol{\theta})$ , since these observations are independent. For more details, we refer to the Bayesian analysis in (Suyu et. al. 2013). We did not consider the lens light due to limitations of the glafic software (Oguri 2010). This would not change the result much according to the H0LiCOW experience since the elliptical galaxy can be well modelled by a Sérsic light model.

We repeated this process 300 times by using different noises added to the observations, i.e., different realizations of the observations. Finally, we calculated time delays based on the best fitted smooth lens model and calculated the standard deviation of all time delays. The histograms are shown in Fig. 3 (b) and (e).

Note that in principle, to infer  $\sigma_{obs}$ , one should perform a MCMC simulation to get the uncertainties for

one noise realization based on perturbed arcs and image positions rather than a smooth model. However, we just need to estimate the scale of  $\sigma_{obs}$  rather than model a specific lensing system. Therefore the average perturbation could be close to zero and the procedure we adopted is reasonable.

### 3.5. Host arc perturbation and $\sigma_{arc}$

Dark matter subhalos change the lensing potential and perturb the observed host arcs. When we fit the arcs based on a certain smooth model, the corresponding systematic errors would occur. To explore the scale of  $\sigma_{arc}$ , we used a similar approach like in  $\sigma_{obs}$ . However, the noise map was added to the perturbed arcs, and then we fitted the smooth model. The resulted uncertainty  $\sigma_{merge}$  should include both  $\sigma_{obs}$  and  $\sigma_{arc}$  and the fitting  $\chi^2$  should be larger than 1 due to unconsidered systematics. Actually, we notice that when studying cosmology, pixel uncertainties were increased so that the  $\chi^2 = 1$  (Suyu et. al. 2013) to avoid systematics.

Since  $\sigma_{obs}$  and  $\sigma_{arc}$  are merged together as  $\sigma_{merge}$ , while the former one is from observational noise, the latter one is from the mismatch between perturbed arcs and a smooth fitting model, we must deduce  $\sigma_{arc}$  from  $\sigma_{obs}$  through  $\sigma_{arc}^2 = \sigma_{merge}^2 - \sigma_{obs}^2$ . We also investigated the covariance between  $\sigma_{dm}$  and  $\sigma_{arc}$  and found that it could be neglected. Local subhalos near the point images primarily affect  $\sigma_{dm}$ , whereas  $\sigma_{arc}$  is affected by all subhalos. They are approximately independent.

We summarize all relative uncertainties in Tab. 3 for the double image system and Tab. 4 for the quad image system.

## 4. DISCUSSION

Study of dark matter substructure using time delay anomaly method is unaffected by dust extinction and stellar microlensing. We proposed to use lensed GW signals accompanied by electromagnetic counterparts to enhance the performance of this approach, which will make it a promising and robust probe.

The very term "time delay anomaly" tacitly suggests the following procedure: fit part of the observational data with a smooth lens model and then compare the inferred time delay with the measured one. If the difference between the two is larger than acceptable (conservative) statistical uncertainty – anomalies occur.

Previous works based on lensed quasars used the information encoded in lensed images assuming a point source to infer the smooth model via Monte Carlo simulation based on certain galaxy catalogs. Moreover, time delay measurements from the light curves had considerable uncertainties. Consequently, the statistical uncertainties were too large comparing with the systematical uncertainty from dark matter. Therefore it was hard to identify the effects of dark matter halos in a reliable manner. As for the anomalies found in RX J1131-1231 and B1422+231 (Congdon et. al. 2010), one could expect that they might be caused by other systematics rather than the dark matter subhalos described in ref. (Keeton & Moustakas 2009). Besides, in previous methods, only quad systems with time delay ratio measurements could be used robustly, due to the radial mass profile degeneracy. The power law slope index could af-

<sup>1</sup> <http://www.stsci.edu/hst/observatory/focus/TinyTim>

Double	A(1)	A(2)	B(1)	B(2)	Quad	A(2)	A(3)	B(2)	B(3)	C(2)	C(3)	D(2)	D(3)
$r(\prime\prime)$	0.021	0.018	0.040	0.037		0.025	0.004	0.021	0.004	0.019	0.003	0.025	0.005

TABLE 2

POSITION DISTANCE PERTURBATIONS FOR ALL IMAGES IN DOUBLE AND QUAD SYSTEMS. X AND Y DIRECTION PERTURBATIONS ARE GAUSSIAN-LIKE, AND  $r = \sqrt{x^2 + y^2}$  IS NON-GAUSSIAN, WE SHOW THE VALUES CORRESPONDING TO THE MAXIMUM PROBABILITIES.

	$\sigma_{dm}$	$\sigma_{obs}$	$\sigma_{merge}$	$\sigma_{arc}$	$\sigma_{stats}$	$\sigma_{sys}$
case 1	1.7%	1.4%	3.7%	3.4%	2.64%	4.75%
case 2	1.34%	1.4%	2.1%	1.57%	2.64%	2.30%

TABLE 3

UNCERTAINTIES FOR DOUBLE IMAGE SYSTEM FOR CASE 1 AND 2.

		$\sigma_{dm}$	$\sigma_{obs}$	$\sigma_{merge}$	$\sigma_{arc}$	$\sigma_{stats}$	$\sigma_{sys}$
case 2	BA	6.3%	0.60%	7.1%	7.07%	2.3%	9.47%
	CA	5.7%	0.58%	6.8%	6.78%	2.3%	8.85%
	DA	4.3%	0.41%	6.0%	5.99%	2.27%	7.37%
case 3	BA	0.95%	0.60%	1.8%	1.7%	2.3%	1.94%
	CA	0.86%	0.58%	1.4%	1.27%	2.3%	1.54%
	DA	0.64%	0.41%	0.9%	0.8%	2.27%	1.03%

TABLE 4

UNCERTAINTIES FOR QUAD IMAGE SYSTEM FOR CASE 2 AND 3.

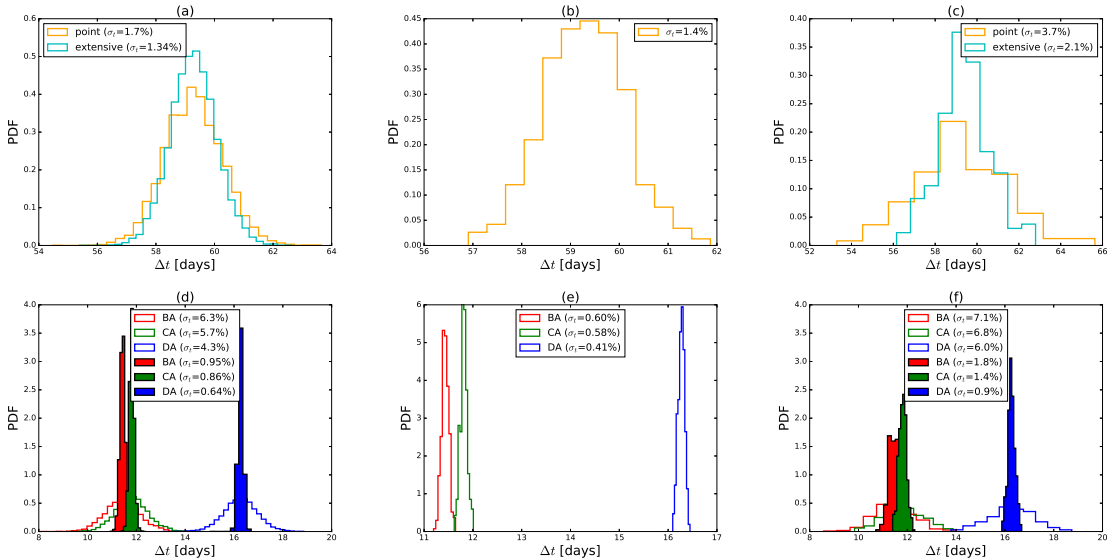


FIG. 3.— Uncertainty results for different mass functions and internal structures case for double and quad systems in case 1, 2, 3. (a)  $\sigma_{dm}$  for double in case 1, 2; (b)  $\sigma_{obs}$  for double; (c)  $\sigma_{merge}$  for double in case 1, 2; (d)  $\sigma_{dm}$  for quad in case 2, 3; (e)  $\sigma_{obs}$  for quad; (f)  $\sigma_{merge}$  for quad in case 2, 3;

fect time delay between two images, but the time delay ratio should be immune to it.

The advantage of the method we propose is that while the lensed quasar could only measure time delay at the percent level through sampled light curves, the lensed GW signal provides a very accurate measurement due to its transient nature. With the improvement of the quality of optical images, we propose to directly extract information about the smooth model from the arcs. Without contamination of the host galaxy image by bright AGN, the lensed GW system identified in the optical, could provide complete host arcs. This would contribute to lens modelling, thus decreasing considerably the value of  $\sigma_{obs}$  as part of statistical uncertainties. Then one might

be able to uncover systematical uncertainties more easily. Our method could test both double and quad systems since it directly fits the lens parameters like the slope parameter to the images and contains no slope-time delay degeneracy. For cusp images, the image order method should be more robust. We also considered the statistical uncertainty brought by cosmology and line of sight fluctuations.

As one can see from Tab. 3 and Tab. 4, under the assumptions we made, statistical uncertainties are  $\sim 2.5\%$  and systematical uncertainties range from 1% to 10%, depending on the dark matter subhalo mass functions, internal structure and lensing configurations. We conclude that systematical uncertainties are comparable to statis-

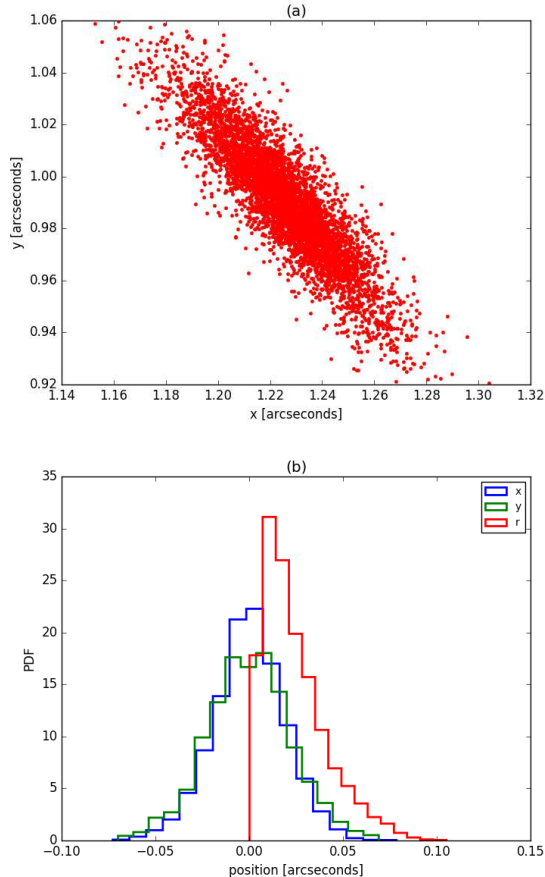


FIG. 4.— Position perturbation for image B in double-image system in case 1. (a) realizations from the same mass function, the orientation is the same as the local arc; (b) x, y and distance perturbations.

tical ones, which is very promising. Concerning lensed quasars,  $\sigma_{obs}$  could be several times larger (Liao et. al. 2017) due to bright AGNs, and one needs also to consider statistical uncertainties from time delay measurements via sampled light curves. These may lead to very large statistical uncertainties compared with systematic ones and in most cases would make dark matter subhalo effects hard to probe.

We emphasize that in this work we only discussed the statistical relationship between mass function and perturbation uncertainties. Actually, one can not get a quantitative result from the measurement of a single system. However, each measurement could provide the lower limit of the substructure according to measured time delay anomalies. With more available systems, dark matter substructure will be assessed more accurately.

On the other hand, we also notice that in many cases, just one or a few subhalos could explain the observed flux anomalies. For example, the satellite in lens RXJ1131-1231 (Suyu et. al. 2013) and the subhalo in lens B1422+231 (Nierenberg et. al. 2014) could fit the observed flux ratios well. For such cases, lensed GW systems would be more powerful and probe these substructures more accurately.

**Throughout this work, we assumed that the dark matter substructure is solely responsible for time delay anomalies. However, there are known**

cases where the large-scale substructure is in the form of disks (Hsueh et. al. 2016, 2017, 2018). When the disks are edge-on oriented, they can also generate flux-ratio anomalies and time delay anomalies as well. Therefore, one should be very careful about the complexity of baryonic structure. It is critical to directly detect the edge-on disks or massive luminous satellites through high-resolution imaging. For example, the Keck adaptive optics or HST imaging may reveal these disks. One may also try to constrain the mass of the disk independently, through kinematic measurements. On the other hand, we need further simulations and emulations to see whether these baryonic structures could be distinguished. Certainly, more complex mass models will have to be considered for a robust quantification of dark matter substructure. In this context, we also refer to the ongoing TDLMC program whose goal is to assess the present capabilities of lens modeling codes and assumptions and test the level of accuracy of cosmological inference. In this program, the team generating mock data will add some systematics to see whether the community could recover them with state-of-the-art modeling techniques.

## 5. PERSPECTIVES

We have demonstrated that the lensed GW signal accompanied by the electromagnetic counterpart could be an excellent tool to study dark matter substructure in galaxies by its accurate time delay measurements. When combined with flux ratio, astrometric and small-scale structure measurements, the dark matter subhalo mass function could be tested. In particular, flux ratios should not be confounded by microlensing due to the long wavelengths of GWs. It is different from the traditional radio loud quasars whose source sizes are extended enough for convolution of the magnification map. The limitation of this method lies in relatively small number of such systems supposed to be detected by third-generation GW detectors, i.e. 2-10 per year for binary neutron stars or neutron-black hole systems with electromagnetic counterparts. The methodology we presented can be also applied in lensed quasar systems, with the caveats discussed above. As for the lensed quasars, the upcoming LSST will bring us  $\sim 400$  systems with well-measured time delays in 10 years (Liao et. al. 2015). One may combine many such lensed quasar systems to improve the measurement precision. However, in such case one should make some statistical assumptions like that the dark matter substructure in all lensed systems is similar. On the other hand, with lensed GW signals individual lenses could be probed better. We look forward to seeing these systems detected and our method applied in studying dark matter substructure.

## ACKNOWLEDGMENTS

K. Liao was supported by the National Natural Science Foundation of China (NSFC) No. 11603015 and the Fundamental Research Funds for the Central Universities (WUT:2018IB012). X. Ding acknowledges support by China Postdoctoral Science Foundation Funded Project (No. 2017M622501). M. Biesiada was supported by For-

eign Talent Introducing Project and Special Fund Support of Foreign Knowledge Introducing Project in China. He also acknowledges hospitality of the Wuhan University. This research was also partly supported by the Poland- China Scientific & Technological Cooperation Committee Project No. 35-4. Z.-H. Zhu was supported by the National Basic Science Program (Project 973) of China under (Grant No. 2014CB845800), the National

Natural Science Foundation of China under Grants Nos. 11633001 and 11373014, the Strategic Priority Research Program of the Chinese Academy of Sciences, Grant No. XDB23000000 and the Interdiscipline Research Funds of Beijing Normal University. X.-L. Fan was supported by NSFC No. 11633001, 11673008 and Newton International Fellowship Alumni Follow on Funding.

## REFERENCES

- Abbott, B. P., et. al. 2016a, *PhRvL*, 116, 061102  
 Abbott, B. P., et. al. 2016b, *PhRvL*, 116, 241103  
 Abbott, B. P., et. al. 2017a, *PhRvL*, 118, 221101  
 Abbott, B. P., et. al. 2017b, *PhRvL*, 119, 161101  
 Abernathy, M., et. al. 2011, European Gravitational Observatory, document number ET-0106A-10  
 Biesiada, M., Ding, X., Piórkowska, A., Zhu, Z.-H. 2014, *JCAP*, 10, 080  
 Cao, Z., Li, L.-F., Wang, Y. 2014, *PhRvD*, 90, 062003  
 Congdon, A. B., Keeton, C. R., Nordgren, C. E. 2010, *ApJ*, 709, 552  
 Diemand, J., Kuhlen, M., Madau, P., et. al. 2008, *Nature*, 454, 735  
 Drlica-Wagner, A., Bechtol, K., Rykoff, E. S., et. al. 2015, 813, 109  
 Ding, X., Biesiada, M., Zhu, Z.-H. 2015, *JCAP*, 12, 006  
 Ding, X., Treu, T., Shajib, A. J., et. al. 2018, arXiv: 1801.01506  
 Ding, X., Liao, K., Treu, T., et. al. 2017, *MNRAS*, 465, 4634  
 Evans, N. W., Witt, H. J., 2003, *MNRAS*, 345, 1351  
 Fan, X., Liao, K., Biesiada, M., Piórkowska-Kurpas, A., Zhu, Z.-H. 2017, *PhRvL*, 118, 091102  
 Fernández, R., Metzger, B. D. 2016, *Annu. Rev. Nucl. Part. Sci.*, 66, 23  
 Gilman, D., Agnello, A., Treu, T., Keeton, C. R., Nierenberg, A. M., 2017, *MNRAS*, 467, 3970  
 Hsueh, J.-W., Fassnacht, C. D., Vegetti, S., et. al. 2016, *MNRAS*, 463, L51  
 Hsueh, J.-W., Oldham, L., Spingola, C., et. al. 2017, *MNRAS*, 469, 3713  
 Hsueh, J.-W., Despali, G., Vegetti, S., et. al. 2018, *MNRAS*, 475, 2438  
 Inoue, K. T., Chiba, M. 2005, *ApJ*, 633, 23  
 Jackson, N., Tagore, A. S., Roberts, C., et. al. 2015, *MNRAS*, 454, 287  
 Klypin, A., Kravtsov, A. V., Valenzuela, O., Prada, F. 1999, *ApJ*, 522, 82  
 Koopmans, L. V. E, Garrett, M. A., Blandford, R. D., et. al. 2002, *MNRAS*, 334, 39  
 Kamionkowski, M., Liddle, A. R. 2000, *PhRvL*, 84, 4525  
 Keeton, C. R., Moustakas, L. A. 2009, *ApJ*, 699, 2  
 Lovell, M. R., Frenk, C. S., Eke, V. R., et. al. 2014, *MNRAS*, 439,300  
 Land, K., Magueijo, J. 2005, *PhRvL*, 95, 071301  
 Liao, K., Treu, T., Marshall, P., et. al. 2015, *ApJ*, 800, 11  
 Liao, K., Fan, X., Ding, X., Biesiada, M., Zhu, Z.-H. 2017, *Nature Communications*, 8, 1148  
 Moore, B., Ghigna, S., Governato, F., et. al. 1999, *ApJ*, 524, 19  
 Mao, S., Schneider, P. 1998, *MNRAS*, 295, 587  
 Mittal, R., Porcas, R., Wucknitz, O. 2007, *Astronomy and Astrophysics*, 465, 405  
 Nierenberg, A. M., Treu, T., Brammer, G., et. al. 2017, *MNRAS*, 471, 2224  
 Nierenberg, A. M., Treu, T., Wright, S. A., Fassnacht, C. D., Auger, M. W. 2014, *MNRAS*, 442, 2434  
 Nakamura, T. T. 1998, *PhRvL*, 80, 1138  
 Oguri, M. 2010, *PASJ*, 62, 1017  
 Piórkowska, A., Biesiada, M., Zhu, Z.-H. 2013, *JCAP*, 10, 022  
 Rusu, C. E., Fassnacht, C. D., Sluse, D., et. al. 2017, *MNRAS*, 467,4220  
 Spergel, D. N., Steinhardt, P. J. 2000, *PhRvL*, 84, 3760  
 Schechter, P. L., Wambsganss, J. 2002, *ApJ*, 580, 685  
 Sereno, M., Sesana, A., Bleuler, A., et. al. 2010, *PhRvL*, 105, 251101  
 Suyu, S. H., Bonvin, V., Courbin, F., et. al. 2017, *MNRAS*, 468, 2590  
 Suyu, S. H., Auger, M. W., Hilber, S., et. al. 2013, *ApJ*, 766, 70  
 Takahashi, R., Nakamura, T. 2003, *ApJ*, 595, 1039  
 Tie, S. S., Kochanek, C. S. 2018, *MNRAS*, 473, 80  
 Treu, T. 2010, *Annu. Rev. Astron. Astrophys.*, 48, 87  
 Vegetti, S., Koopmans, L. V. E. 2008, *MNRAS*, 392, 945  
 Wayne, W., Barkana, R., Gruzinov, A. 2000, *PhRvL*, 85, 1158  
 Wang, Y., Stebbins, A., Turner, E. L. 1996, *PhRvL*, 77, 2875  
 Wong, K. C., Suyu, S. H., Auger, M. W., et. al. 2017, *MNRAS*, 465, 4895  
 Xu, D., Sluse, D., Gao, L., et. al. 2015, *MNRAS*, 447, 3189  
 Zackrisson, E., Riehm, T. 2010, *Advances in Astronomy*, 2010, 478910